FLOOD ALERT SYSTEM USING HIGH RESOLUTION RADAR DATA IN THE MAYAGUEZ-PUERTO RICO BAY DRAINAGE BASIN

69

LUZ ESTELLA TORRES MOLINA*
Department of Civil Engineering, Universidad del Turabo, Gurabo, Puerto Rico.

SANDRA CRUZ-POL AND JOSE COLOM
Department of Electrical and Computer Engineering, University of Puerto Rico-Mayagüez.

ABSTRACT

Flash floods are considered one of the most unpredictable and costly natural disaster event caused by precipitation. It is important to achieve a trustful forecast in order to help mitigate a major disaster. This task is even more challenging when considering a tropical and complex terrain environment. This current work is a first assay to introduce a Flood Alert System in the western region of the tropical island of Puerto Rico. The main tool is the use of recently installed X-band weather radars, which provide high temporal and spatial resolution rainfall data. High resolution is essential in developing a forecasting model for convective precipitation for time periods of a few hours or less (defined as nowcasting by the WMO).
The accuracy of these forecasts generally decreases very rapidly during the first 30 min because of the very short lifetime of individual convective pixels. A number of observational studies have shown that individual convective cells have mean lifetimes of about 20 min, with the best performance associated with a lead-time of 10 min. Numerical simulation studies have contributed significantly to the understanding of storm composition and duration; this is just beginning to be recognized in currents nowcasting systems. The nowcasting technique developed in this work is a special kind of nonlinear model with stochastic and deterministic components. The rainfall forecasts obtained using the considered method is then routed through a rainfall runoff model (*Vflo*™).

1. INTRODUCTION

Portions of western Puerto Rico are subject to flash flooding due to sudden, extreme rainfall events, some of which fail to be detected by the only NEXRAD (WSR-88D) radar on the island, located approximately 120 km away and partially obstructed by mountains. The use of new radars with higher spatial resolution and covering areas missed by the NEXRAD radar, are important for flood forecasting efforts, and for studying and predicting atmospheric phenomena.

NEXRAD coverage has limitations in observing below 10,000 feet or 3 kilometers (called the Gap) above sea level for the Mayagüez area and nearby towns [*Cruz-Pol et al.*, 2011]. At these locations, NEXRAD cannot "see" if raindrops are forming within the Gap, resulting in a different rain rate than other radars which can measure the lower portion of the cloud, see Figure 1.

Recently, the University of Puerto Rico in Mayagüez Campus [*Trabal et al.*, 2011] developed a weather radar network using two (2) types of radars, namely: Off-the Grid (OTG) and TropiNet, with radius of coverage of 15 km and 40 km, respectively. This network is capable of monitoring the lower atmosphere, where most atmospheric phenomena occur. Both radar systems are short-range and high frequency (X-band), compared to NEXRAD. This allows for high spatial (60m versus 1km for NEXRAD) and temporal resolution (less than 1 min versus 6 min for.NEXRAD.) This work represents the first time that TropiNet radar technology was used for hydrologic analyses and specifically for rainfall forecasting in western Puerto Rico.

* *Corresponding author address:* Luz E. Torres-Molina, Univ. del Turabo, Dept. of Civil Engineering, Gurabo, PR 00778-3030; e-mail: TORRESL6@suagm.edu

Short-term rainfall forecasts have commonly been made using Quantitative Precipitation Forecast (QPF). The introduction of quantitative precipitation forecasting (QPF) in flood warning systems has been recognized to play a fundamental role.

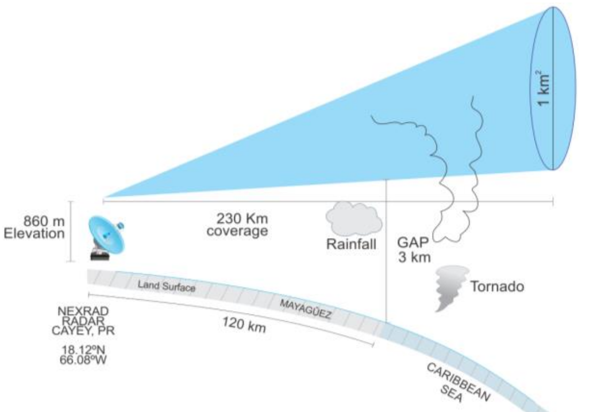

Figure 1. Long range problem with NEXRAD [based on Westrick et al., 1999]. The figure does not include topography of the land surface.

QPF is not an easy task, with rainfall being one of the most difficult elements of the hydrological cycle to forecast [*French et al.*, 1992] and great uncertainties still affect the performances of stochastic and deterministic rainfall prediction models [*Toth et al.*, 2000].

Currently, this capability does not exist in western Puerto Rico, and it is needed because of the high potential for flooding in certain areas (e.g., in flood plains near the principal rivers of the region). In this research, short-term rainfall forecast analysis is performed using nonlinear stochastic methods. Once obtained, the rainfall forecast is introduced into a hydrologic/inundation model *Vflo* and into the Inundation Animator configured for the Mayagüez Bay Drainage Basin (MBDB). Specific components of the research are: the inclusion of calibration and validation of rainfall estimates produced by the TropiNet radar network, the development and validation of the stochastic rainfall prediction methodology, the calibration and validation of the inundation algorithm at selected locations within the MBDB, and the proto-type of an operational, real-time flood alarm system for the MBDB. The proto-type, automated Flood Alarm System (FAS) will be able to send near-real time updated inundation images to a website on the Internet.

2. STUDY AREA

The study area encompasses the MBDB, is 819.1 km^2 in size [*Rojas*, 2012] and is located in western Puerto Rico. The region has three (3) important watersheds: Río Grande de Añasco, Río Guanajibo and Río Yagüez. The area includes twelve (12) municipalities: Mayagüez, Añasco, Las Marías, San Sebastián, Lares, Maricao, Yauco, Adjuntas, Sabana Grande, San Germán, Hormigueros and part of Cabo Rojo. These three important rivers discharge into Mayagüez, Añasco and Cabo Rojo branches, respectively. According the U.S. Census Bureau Mayagüez has 89,080 habitants and a total area of approximately 143.53 km^2 of which about 25.20 km^2 are in flooding areas, Añasco has 29,261 habitants with a total area of about 102.82 km^2 and 23.11 km^2 are in flooding areas, and Cabo Rojo has 50,917 habitants with a total area of about 187.81 km^2 and 44.42 km^2 are in flooding area [*U.S. Census Bureau*, 2010], see Figure 2.

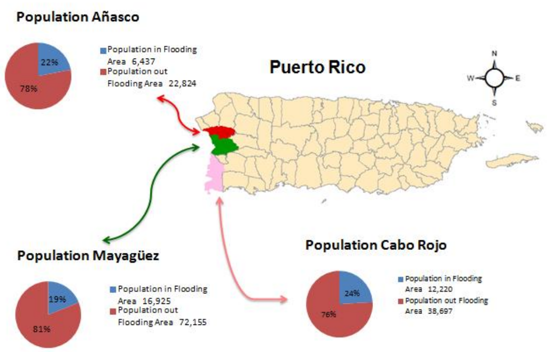

Figure 2. Population lives in floodable areas, U.S. Census Bureau, 2010.

The basin of the Río Grande de Añasco has an area of 467.7 km^2 of which approximately 10 percent of the area is flat land and the other remaining 90 percent is mountainous. The floodplain covers approximately three-fourths of the flat land, and the residential developments in the Añasco municipality are partially within this area, and therefore can be affected by flooding. Río Grande de Añasco flows westerly 74 km to the coast where its discharges into the Bay of Mayagüez. Changes in elevation are shown in Figure 3 and vary from zero meters at mean sea level in the coastal areas to 960 meters in the mountainous areas.

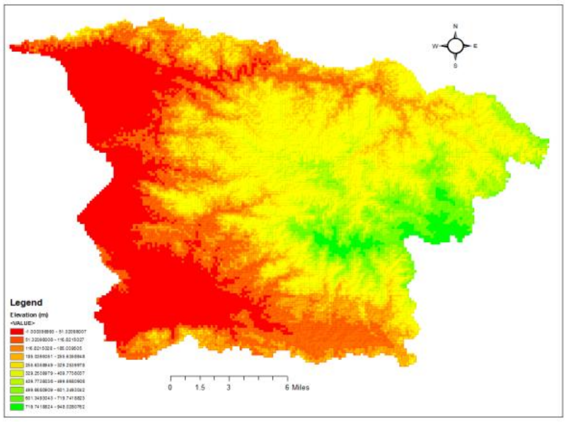

Figure 3. Digital Elevation Model.

3. SOIL CLASSIFICATION

The soil map was provided by United States Department of Agriculture – Natural Resources Conservation service (USDA-NRCS).

The soil textures present in this study as percent of area are clay with 62.49%, clay–loam 24.96%, rock 8.69%, loam 3.00%, sand 0.81% and gravel 0.04%. A soil map describing the class distribution is necessary to assign the values the Green-Ampt infiltration parameters, see Figure 4

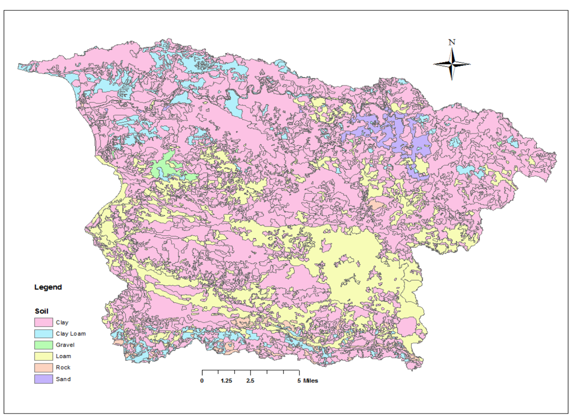

Figure 4. Soil Present in the study area. [Source: Soil Survey Geographic (SSURGO)].

Twenty (20) different classes of land cover and forest type are present over the study area corresponding to different kind of forest, woodland and agriculture. The classification of land cover in this model is used to assign values for physical based parameters which are important in the simulation with *Vflo*, other important parameters with the land use are manning's roughness coefficient, rainfall interception, evapotranspiration, crop coefficient and other.

4. HIGH RESOLUTION RAINFALL RADAR PRODUCT

Commonly, the flood alert systems have fulfilled the role of providing flood notification to many people and have saved lives and properties. However, many alert systems fail due to low precision of the models and the sudden change of the atmosphere. One of the greatest sources of uncertainties in the prediction of flooding is the rainfall input.

NEXRAD has been used by the NWS to estimate rainfall in Puerto Rico. The NEXRAD facility for Puerto Rico is located near the City of Cayey at 860 m above mean sea level and at approximately 120 km from Mayagüez city. The location of radars provides full nationwide coverage over the contiguous United States at a specified height above each of the individual radars, but this may present a problem in the western Puerto Rico due to the distance from the NEXRAD radar and topography of the Island. Currently, the Puerto Rico Weather Radar Network (PRWRN) administrated by UPR-Mayagüez has three (3) polarimetric TropiNet radars. The TropiNet radars are Doppler dual-pol radars which allow the radar beam to measure reflectivity close to the ground, overcoming the shadow effect of the Earth's curvature, while maintaining high range and azimuth. They have high space and time resolution for weather monitoring and detection, and are capable of generating very high resolution data with a range of 40 km of radius or maximum radial distance (horizontal range) of 80 km of diameter. The spatial resolution is very high if this is compared with NEXRAD radar (60 m versus 1 km). The study area coverage is 940x740 radar pixels and its temporal resolution is 1-minute.
To analyze the data it was necessary to develop a model to convert raw data to NetCDF data and then convert the reflectivity data in dBZ to rain-rate in (mm/hr) using empirically derived *Z-R* relationships. *Marshal and Palmer* [1948] equation is the default *Z/R* relationship employed by the NEXRAD and TropiNet.

5. STOCHASTIC MODELING OF SHORT-TERM RAINFALL

For atmospherics phenomena it is difficult to predict deterministically what will occur in the future. A mathematical expression which describes the probability structure of the time series that was observed due to the phenomenon is referred to as a stochastic process. The precipitation is an example of stochastic phenomenon that evolves in time according to probabilistic laws. A time series model is adapted to a series in order to calibrate the parameters of stochastic process. Stochastic models are able to provide reliable predictions over small temporal and spatial scales, which are interested in hydrological applications.

An algorithm for predicting 10, 20 and 30 min in advance the spatial distribution of rainfall rate is introduced in this work. The algorithm is based on the fact that TropiNet radar rainfall-rate data provides estimations of the rainfall with high spatial and temporal resolution. The suggested algorithm uses TropiNet (RXM-25) data to predict the variability of the rainfall field in time and space. It is assumed that for a short time period, (10, 20 and 30 min) a rain cloud behaves as a rigid object, with all pixels moving in the same direction at a constant speed. Thus, the most likely future rainfall areas are estimated by tracking rain cell centroid advection in consecutive radar images. The suggested algorithm is a special kind of nonlinear model with stochastic and deterministic components. The rainfall process exhibits significant changes in time and space, and it can be characterized as a non-stationary stochastic process. To face the nonstationary characteristic of the process, parameters are estimated at every time and spatial domain.

The model consists in considering the rainfall shape data as a rectangular grid with 940 columns and 740 rows of pixels for a total of 695,600 pixels, every pixel size is 0.06 kilometers wide and 0.06 kilometers long. From the grid data select a zone of 81 pixels that was divided in squares of $\Delta x \times \Delta y$ pixels, where (Δx) is referenced to columns of 9 pixels and (Δy) rows of 9 pixels with total zones of 8528 ($82x104$) in every window, as shown in Figure 5. Several zones sizes were explored for $\Delta x \ and \ \Delta y = \{7, 9, 11, \ldots, 25\}$ and it was found that the larger the zone size, the larger the number of degree of freedom. However, resolution was degraded with increased zone size.

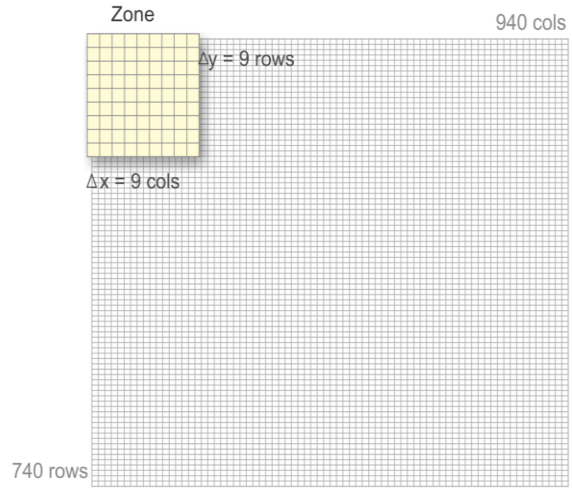

Figure 5. Rectangular grid of rainfall data.

In the model, the use of the same zone in the before windows $(t-1)$ and $(t-2)$ is necessary, see Figure 6. Every zone (9x9) should have a minimum of twenty four (24) rain pixels with twenty (20) degrees of freedom. Zones with less pixel of rain could not be selected to forecast analysis. In zones where the prediction movement suggest there is a rainfall cell but the zone has not the necessary pixels required (24 pixels) an interpolation was applied. The interpolation was "*Kriging simple*" using the twenty five (25) pixels nearest to pixel that has no prognostic.

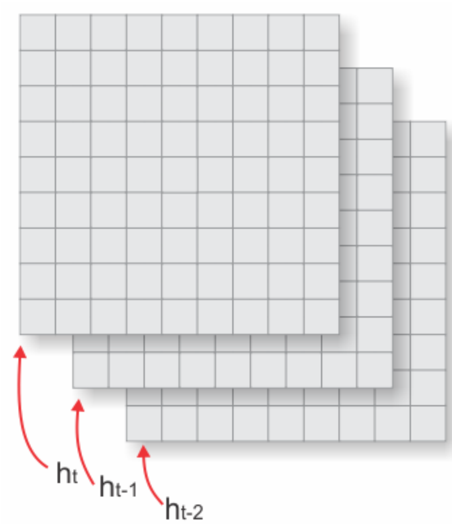

Figure 6. Zone 9 x 9 at time *t*-1 and t-2.

The model is defined by the equation

$$h_{t,k(i,j)} = \alpha_{t,k} + (\beta_{t,k} - \alpha_{t,k})\Phi_{t,k}\left[1 - e^{-\Sigma\left(\delta 1_{t,k}\bar{h}_{t-1,k(i,j)} + \delta 2_{t,k}\bar{h}_{t-2,k(i,j)} + \delta 3_{t,k}Z_{t-1,k(i,j)}\right)}\right] + \varepsilon_{t,k(i,j)} \quad (1)$$

where (i, j) represents the geographic position or coordinates latitude and longitude of every pixel in the grid, k is the zone. This process starts in pixel 1 until pixel 8528. In every zone, unknown parameters should be determined $(\alpha, \beta, \Phi, \delta1, \delta2, \delta3)$: α is the minimum value found between previous values of $h_{t-1,k(i,j)}$ and $h_{t-2,k(i,j)}$ in their respective zones (k), β is the reflectivity maximum value found between previous values of $h_{t-1,k(i,j)}$ and $h_{t-2,k(i,j)}$ in the specific zone (k).

The mathematical structure of the model was developed from previous work [*Ramirez-Beltran et al.*, 2008]. In the current work, this model was used because this scheme ensures that rainfall forecasts will fall inside of the most likely rainfall intensity domain $[\alpha, \beta]$, which was derived by the observed local rainfall distribution.

$\bar{h}_{t-1,k(i,j)}$ is the reflectivity average value in the time $(t-1)$. The average value was determined in every pixel into each zone. It was obtained averaging the eight pixels closest to the pixel under study. Similarly, $\bar{h}_{t-2,k(i,j)}$ is the average reflectivity value in the time $(t-2)$, see Figure 7.

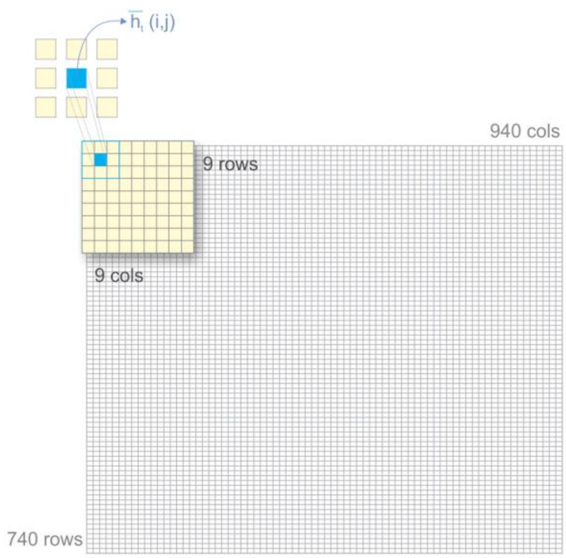

Figure 7. Average pixels at a specific zone using the eight nearest pixels.

The variable $Z_{t-1,k(i,j)}$ is the ratio between the pixels with maximum reflectivity. $Z_{\max(t-1),k(i,j)}$ in every cloud or cell and the nearby pixels $Z_{\mathrm{i}(t-1),k(i,j)}$ forming the cloud or cell and the random variable $\varepsilon_{t,k(i,j)}$ is a sequence of an unobserved random variable with mean zero and constant variance associated to the pixel (i, j).

The variable Phi $(\Phi_{t,k})$ is changing in the equation every zone (9x9) in each window. This variable was determined first by linearization of the nonlinear equation (Phi-initial) and after using optimization nonlinear techniques with constrains "*Sequential Quadratic Programming*" (SQP), where the Phi parameter is a bias correction factor and its maximum value must not exceed 1.1. The initial coefficient deltas $(\delta1, \delta2\ and\ \delta3)$ were obtained through the estimation method "*least squares*" by linearization of nonlinear equation (exponential). Once the variables initial deltas were found, the next step is to find the variable Phi $(\Phi_{t,k})$ initial. These values were used to forecast rainfall at one (1) lead-time and successively with the following forecasts.

The motion algorithm was based on a spatial and temporal comparison, classifying clouds with high reflectivity and removing pixel with very low reflectivity, in this work the minimum reflectivity was 3 dBZ. The next step is the normalization of reflectivity values between a range of 0 and 1 using minimum and maximum values of reflectivity in each image or windows, as shown the equation (2), where N_r is the normalized reflectivity, Z_i reflectivity in each pixel, Z_{min} minimum reflectivity 3 dBZ and Z_{max} is the maximum reflectivity in the window. Derivation of the cloud motion vector requires tracking cloud rainfall cells [*Ramirez-Beltran et al.*, 2014].

$$N_r = \frac{Z_i - Z_{min}}{Z_{max} - Z_{min}} \qquad (2)$$

The classification of the normalized values is divided into two groups. This result was stored in a binary matrix B_r. The value N_r exceeding the percent of pixel with a minimum reflectivity $N_{r,min}$ is assigned value of one (1) and the value N_r that is smaller than the percent of pixel with a minimum reflectivity $N_{r,min}$ is assigned the value of zero (0). In this case, $N_{r,min}$ is 10 percent of pixels with values of minimum reflectivity [*Ramirez-Beltran et al.*, 2015].

$$B_r = 0\ if\ N_r < N_{r,min} \qquad (3)$$

$$B_r = 1\ if\ N_r \geq N_{r,min} \qquad (4)$$

To estimate the initial values of deltas, application of a constrain was not necessary, therefore the initial deltas values can be positives or negatives. The main equation was linearized by considering values of

$h_{t,k\,(i,j)}$, $\bar{h}_{t-1,k\,(i,j)}$, $\bar{h}_{t-2,k\,(i,j)}$, $\alpha_{t,k}$, $\beta_{t,k}$ and $Z_{t-1,k\,(i,j)}$ and the unknown values of $\delta 1_{t,k}, \delta 2_{t,k}, \delta 3_{t,k}$, left the parameter phi $\Phi_{\mathrm{t,k}}$ temporarily ignored.

This method consists in solving the equivalent linear model and using these values as the initial point. The convergence of nonlinear routine heavily depends on the selections of the initial points. Thus, if the initial point is far away from the optimal solutions the algorithm may converge to a suboptimal point or may not converge. [*Ramirez-Beltran et al.,* 2015] and [*Torres*, 2014].

6. HYDROLOGIC MODEL

The hydrologic model used in this research is *Vflo* [*Vieux and Vieux*, 2002]. *Vflo* is a fully distributed physically based hydrologic (PBD) model capable of utilizing geographic information and multi-sensory input to simulate rainfall runoff from major river basins to small catchments, see Figure 8.

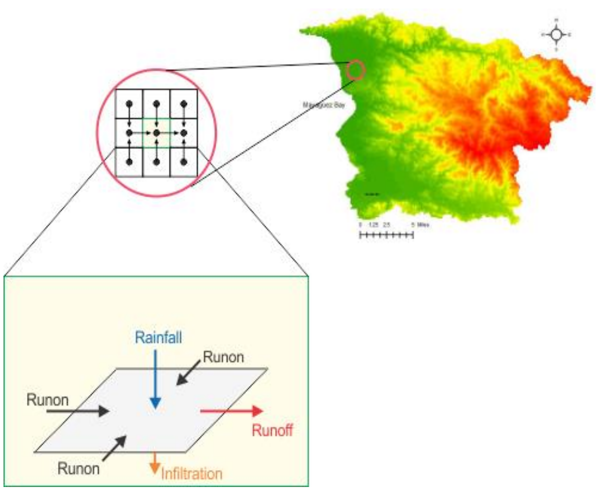

Figure 8. Detailed GIS grid runoff in the watershed.

Vflo is a hydraulic approach to hydrologic analysis and prediction. Overland flow and channels are simulated using the Kinematic Wave Analogy (KWA). The model utilizes GIS grids to represent the spatial variability of factor controlling runoff. Runoff production is from infiltration excess and is routed downstream using kinematic wave analogy. Computational efficiency of the fully distributed physics-based model is achieved using finite elements in space and finite difference in time. *Vflo* is suited for distributed hydrologic forecasting in post-analysis and in a continuous operation mode, derives its parameters from soil properties, land use and topography and, in this case the precipitation, is obtained from the TropiNet radar. The goal of distributed modeling is to better represent the spatial-temporal characteristics of a watershed governing the transformation of rainfall into runoff.

There is a sequence called the "Ordered Physics Based Parameters Adjustment" (OPPA) method developed by *Vieux and Moreda* [2003]. The calibration process (OPPA) approach include estimates of the spatially distributed parameters from physical properties, assigns channel hydraulic properties based on measured cross-sections where available, studies model sensitivity for the particular watershed, and identifies response sensitivity to each parameter. Furthermore, it runs the model for a wide range of storms, from small to large events.
It was fundamental to study the physical configuration of the watershed, such as a Digital Elevation Model (DEM), the digitized topography, soils map, land use map and information about the basin. Some hydrologic and hydraulic studies by U.S Geological Survey - Current Water Data for Puerto Rico [2014] and FEMA [2012] are used in this research as additional information. Some stations from the USGS were used to compare and validate the runoff with the results from the hydrological model using radar data.

Additionally, a GOES satellite-based potential evapotranspiration (PET) product, with resolution of 1 km over the entire island each day, was used in this research. The hydrological *Vflo* model uses PET in units of mm/hr and the same resolution as the Digital Elevation Map in the current study. A subroutine was developed to change the resolution of the PET data from 1 km to 200 meters, and the units from (mm/day) to (mm/hours).

The infiltration is an important parameter to be able to estimate the runoff. The runoff is caused only when the rainfall rates exceed infiltration rates. The hydrologic model use Green-Ampt infiltration routine to model infiltration. Other characteristic parameters in the infiltration process are necessary: Hydraulic conductivity, wetting front, effective porosity, soil depth, initial saturation, abstraction and impervious area, these variables are affected by land use and soils properties.

7. EVENTS SELECTION

To select the events, it was necessary to analyze every storm measured by the radars during 2012 and 2014. It was necessary to determine that the radar data had not interruptions or was damaged. If the radar had corrupt data, the storm is discarded. Table 1 includes the dates and duration of every storm to the current research.

The analysis had important previous steps, the first was taking every minute data from TropiNet radar and determine that the radar data had not interruptions or was damage. If the radar had corrupt data, the storm is discarded.

The next step was to select the radar dataset with the same elevation angle (3˚). The TropiNet radar has the capacity to store data with two or more different elevations angles. The final step was to choose those precipitations that have data with complete storm duration.

Table 1. Characteristics of studied storms

Date	Duration (UTC)
March 28, 2012	7 hr. 16:27-23:58
March 29, 2012	6 hr. 00:36-06:53
April 30, 2012	5 hr. 17:55-22:21
October 10, 2012	5 hr. 16:10-21:43
February 12, 2014	7 hr. 16:00-23:29
May 06, 2014	7 hr. 16:45-23:59
May 21, 2014	7 hr. 16:46-23:00
June 29, 2014	5 hr. 17:00-22:00
June 30, 2014	4 hr. 16:00-20:15
July 05, 2014	4 hr. 16:44-20:00

8. RESULTS

The NEXRAD pixels have 1 km^2 area and the TropiNet pixels have 60 meter for each side (0.0036 km^2 area), this means that 256 TropiNet pixels equivalent in size to one (1) NEXRAD pixel. So within one NEXRAD pixel there are 256 TropiNet pixels. Figure 9 presents a comparison image on a specific minute between TropiNet and NEXRAD.

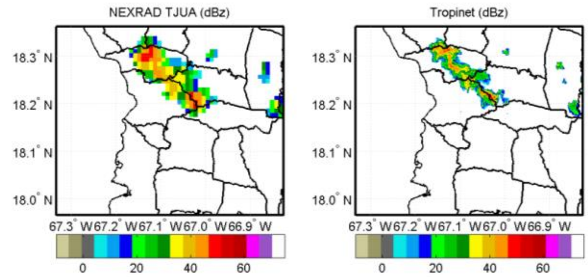

Figure 9. Comparison TropiNet and NEXRAD on May 06, 2014-17:42.

Figure 10 presents one of many comparisons between Rain Gauge, NEXRAD and TropiNet with the original resolution at rain gauge station designate as C1 with latitude 18.2094˚ and longitude 67.1401˚, date May 06, 2014. TropiNet with the original resolution (60mx60m) presents a rain rate data with more appropriate values at C1 stations, considering rain gauge observations as the true values. This is possible due to proximity of TropiNet's beam to the land surface and its high resolution data.

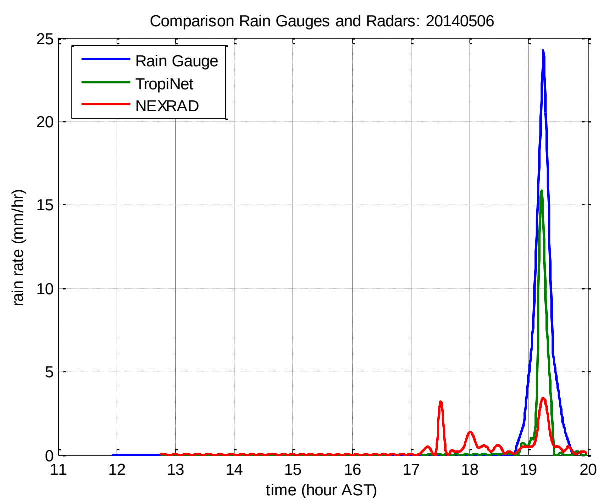

Figure 10. Comparison Rain Gauge-NEXRAD and TropiNet at station C1, on May 06, 2014 (Moderate Rain) with original resolutions data for TropiNet and NEXRAD.

In western Puerto Rico sudden precipitations events occur with very short durations due to the atmospheric conditions and topographic features of the region. Precipitation events may develop, occur and dissipate in periods as short as 1, to 3 hours.

Knowing the precipitation characteristics, the nowcasting model developed in the current research only needs two lag times for prediction. This means that the model has the capacity to forecast the rainfall even if the duration is very short. The developed model is presenting the best prediction when the lead-time is 10 min. The postulated rainfall nowcasting algorithm involves two major tasks: a) predicting the future location of the rain pixels, and b) predicting rainfall at each pixel.

Figure11 presents the sequence of event during 40 min considering each ten 10 min of cloud motion within a total duration event of 7 hours where t_o=16:50 hr, on March 28, 2012.

For all events, the best results were presented with a prediction of 10 min. Western Puerto Rico area geographical position makes it susceptible to sudden rainfalls that are changing rapidly in time and space. Due to this change, a lead-time of 10 min is the time prediction more adequate to this precipitation class. A larger lead-time results in greater statistical errors. Contrarily, using a lead-time smaller than 10 min the purpose of flood alert system will be annulled by the absence of time to evacuation.

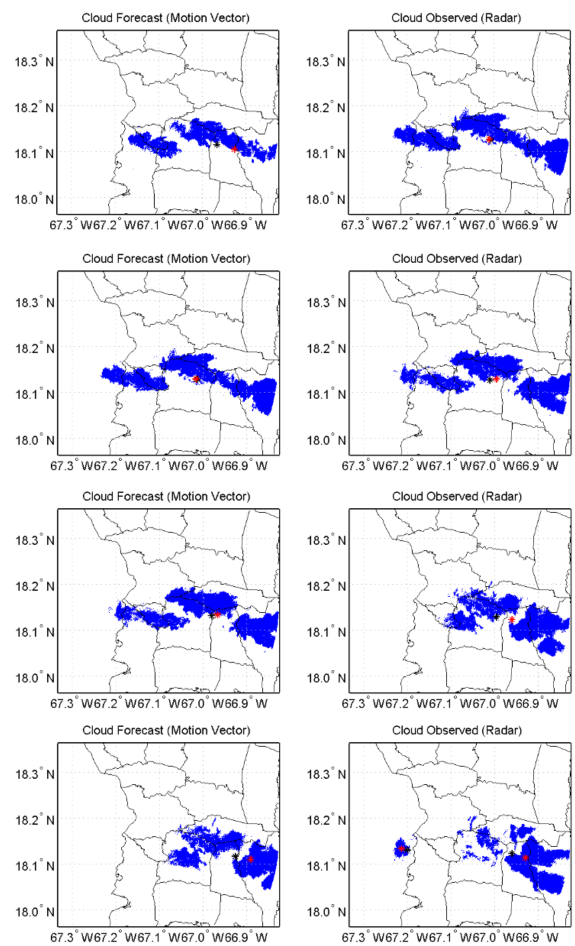

Figure11. Cloud motion sequence with a lead-time of 10 min.

Rainfall is estimated in each pixel within every zone. Thereby, the suggested regression model was developed under the following assumption: It is expected that in a short time (10 min) period a rain cloud behaves approximately as a rigid object and the cloud rain pixels moves in a constant speed and direction. Thus, the most likely future rainfall areas can be estimated by using the advection of the centroids of the rain cells in consecutive images. The current estimation reflectivity is a function of the previous reflectivity images observed. Rainfall nowcasting algorithm task is predicting rainfall rate at each pixel.
The comparison of estimated or predicting reflectivity using the main Equation (1) and observer reflectivity at each pixel were furthermore performed. Figure12 shows the comparison with a lead-time of 10 min where t_o=16:50 hr, on March 28, 2012.

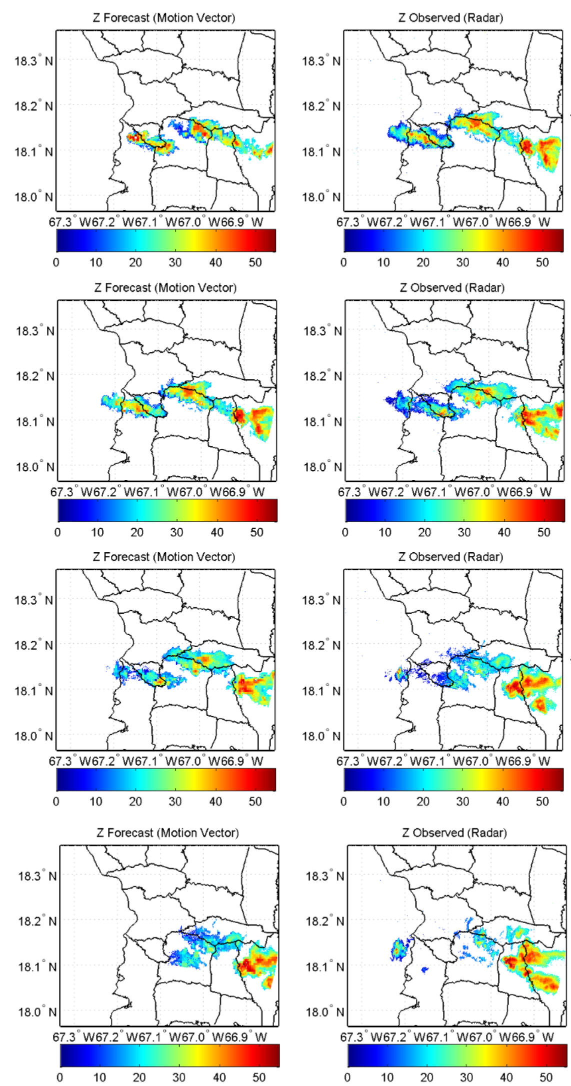

Figure 12. Reflectivity sequence with a lead-time of 10 min.

An analysis for the nowcasting requires a combination of meteorological and hydrological statistics. This allows for a better understanding of the behavior of the spatial and temporal accuracy of the storm prediction. A good nowcasting includes accuracy of the spatial, as well as in the temporal level and accuracy of the predicted rainfall intensity.

Model performance criteria for the prediction required quantitative comparison measurements; these measurements include ten (10) storms. The accuracy of rainfall prediction of each pixel can be measured by decomposing the rainfall process into sequences of discrete and continuous random variables.

Some attributes are related with the contingency table, hit rate (*HR*) is the ratio of correct forecasts to the number of times this event can occurred. Other attribute is the probability of detection (*POD*) as the fraction of those occasions when the forecast event occurred on which it was furthermore forecasted, in this case it is the probability that rain occur. The False Alarm Ratio (*FAR*) is the relation of the forecast events that fail to materialize; the best possible *FAR* is cero and the worst possible *FAR* is one.

For lead-times of 10, 20 and 30 min the storms provide an average hit rate (*HR*) of 0.90, 0.86 and 0.84, respectively. The probability of detection (*POD*) of storms varies from 0.61, 0.50 and 0.41. While the false alarm rates (*FAR*) is 0.27, 0.38 and 0.46 for lead-time of 10, 20 and 30 min, respectively.

Figure13 shows *POD* values and *FAR* values for the complete set of storms. In the ideal situation *POD* should approach to one (1), while the *FAR* results should approach to zero (0).

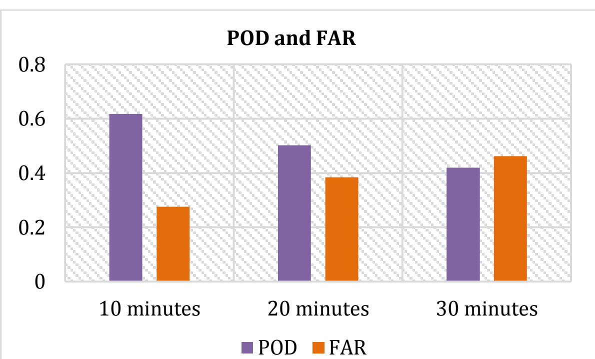

Figure13. Probability of detection and false alarm for the all storms.

For lead-times of 10, 20 and 30 min the storms provide an average hit rate (*HR*) of 0.90, 0.86 and 0.84, respectively are shown Figure14. The hit rate score is the fraction of observed events that is forecast correctly. It ranges from zero (0) at the poor end to one (1) at the good end. The Root mean square error (*RMSE*) and Bias ratio (*BR*) measure the accurate of the simulation for all ten (10) studied. The *RMSE* average values are 0.026, 0.077 and 0.144 mm and the Bias average values are 0.97, 0.98 and 1.04 for lead-times of 10, 20 and 30 min respectively.

The estimation Bias ratio for a lead-time of 30 min presents an average over estimation prediction, while the estimation Bias ratio for a lead-time of 10 min and 20 min show sub estimation. The Bias ratio for the three lead-times is near to one, this mean that they are good estimates [*Pielke*, 1984].

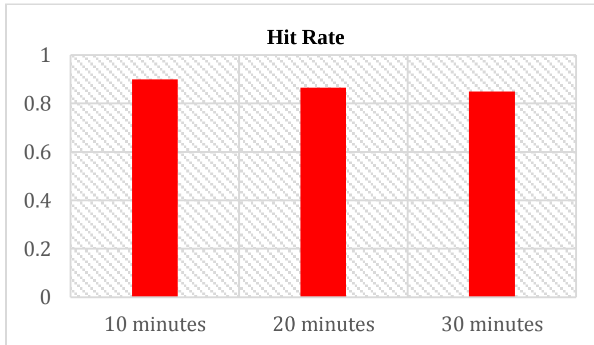

Figure14. Hit rate for the all storms.

The *RMSE* average in 10 min lead-time presents the best result compared with the other lead-time of 20 min and 30 min. The *RMSE* is increasing due to the fact that large errors are occurring because the lead-time is increasing.

Figure 15 show the average rainfall for all rain pixels during each time interval (10 min) for the event on March 28, 2012. In the Figure 15, a time shift is observed. This is due to cloud velocity movement. The time shift could be estimated in the future if additional atmospherics data were available. In general, the mean time shift depends of the storms' lead-time.

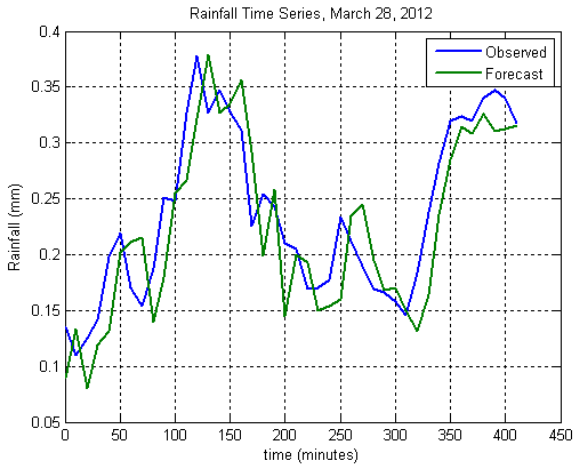

Figure 15. The average rainfall for all rain pixels in each time interval with lead-time of 10 min on March 28, 2012. The blue line represents the observed data (TropiNet) and the green line represents the forecasted data accumulated precipitation for all rain pixel along the total storm event.

Figure16 present for the event on March 28, 2012. It is the accumulated average rainfall for all rain pixels during the total event. It was calculated taking the rainfall total during the storm and the precipitation total area.

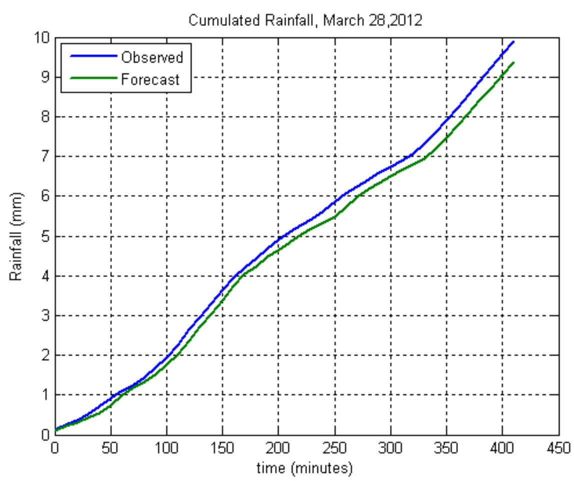

Figure16. The accumulated precipitation average for all rain pixels during whole event on March 28, 2012. The blue line represents the observed precipitation and the green line the forecast.

Figure17 present the scatter plot at the same rainfall event.

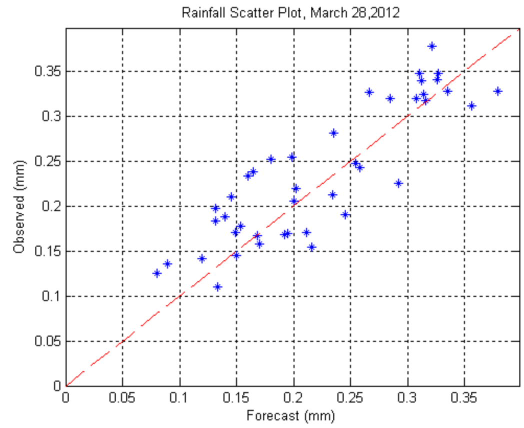

Figure 17. The scatter plot of the forecast event on March 28, 2012.

The Hydrological model *Vflo* required the ensemble of various layers that perform the physical and topographic characteristics of the basin area. These layers are formed by parameters as: effective porosity, hydraulic conductivity, wetting front, roughness, soil depth, and initial saturation which can be most sensitive in the watershed. Spatially distributed parameter and input from radar rainfall requires new methods for adjustment in order to minimize differences between simulated and observed hydrographs. The hydraulic roughness (n), hydraulic conductivity (K) and initial saturation (θ) are the most sensitive parameters of the hydrological model. These values are estimated from physical properties of the watershed adjusted to reproduce system behavior [*Vieux and Moreda*, 2003]. The hydraulic conductivity controls the total amount of water that will be split into the surface runoff. The hydraulic roughness affects the peak flow and the time to peak and initial saturation is related with the existing humidity into the soil.

Scalars are multiplied by these parameter maps to adjust the value in each grid cell while preserving the spatial heterogeneity. The sequence of adjustment was recommended by *Vieux and Moreda* [2003] to minimize the objective function for volume, and then peak flow, obtaining an overall optimal parameter set for the storms.

The reference hydrographs were developed from point observations or observed data of USGS stations numbers: #50144000 at Rio Grande de Añasco (San Sebastián), #50136400 at Rio Rosario (Hormigueros) and #50138000 at Rio Guanajibo (Hormigueros) (U.S Geological Survey -Current Water Data for Puerto Rico [2014]) and compared with results from the hydrological model.

Several adjustments parameters were made as necessary to produce consistent results at the USGS stations compared with every storm. The watershed parameters were adjusted upstream of the observed point (USGS flow stations) by the adjustment method described by *Vieux and Moreda* [2003]. They employ a scalar to adjust parameter maps so that the proposal scalar magnitudes change while the spatial variation is preserved. The scalar used to multiply the n, K and θ parameter maps area defined as follows [*Gourley and Vieux*, 2005].

Study model sensitivity was done for the watershed to identify response sensitivity for peak flow to each storm changing the multiplicative factor in the parameters. The events evaluated were 10 events. A list of parameter ensembles is created for each storm in every station as shown in Figure 18. A total of 450 simulations were done for this analysis.

A compilation of individual simulations are determined based on comparison with the observed stream flow data from (U.S Geological Survey -Current Water Data for Puerto Rico [2014]). The hydrologic evaluation consist of making multiples runs, setting the sensitive parameters in each event, yielding the best simulation between observed data from USGS and estimated data from the nowcasting model. The matching of both peaks in every storm was successfully accomplished with flow values.

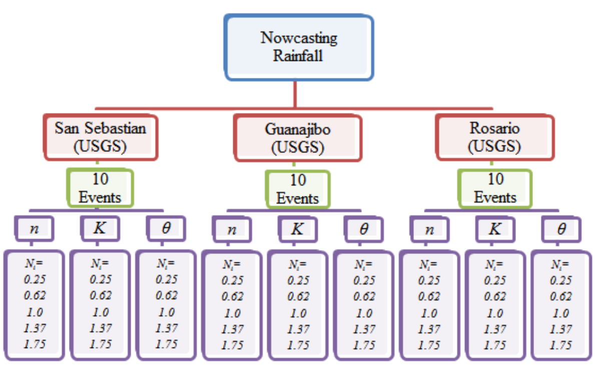

Figure 18. Flow chart of the calibration factor panel for peak flow.

The separation base flow method used in the USGS stations was the straight line method. It is achieved by joining with a straight line the beginning of the surface runoff to a point on the recession limb representing the end of the direct runoff. Comparison results indicate that the nowcasting model is capable of estimating hydrographs at distributed positions within a watershed based on knowledge of hydrographs at USGS stations. The hydrograph shape is observed with high accuracy, with rising and falling limbs, and hydrograph peaks timed well. Small adjustment between 0.8 and 1.20 were present in the calibration factor. Figure19 presents the hydrograph of observed data from the San Sebastian USGS station compared with the simulated results using the nowcasting approach in the hydrological model *Vflo*.

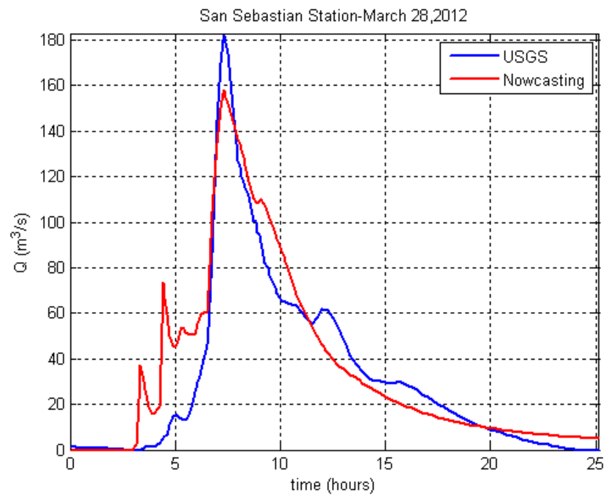

Figure 19. The runoff observed data (USGS) blue line and simulated data (Nowcasting) red line at San Sebastián station on March 28, 2012.

Figure 20 shows the runoff observed data from USGS and the runoff estimated data using the nowcasting results.

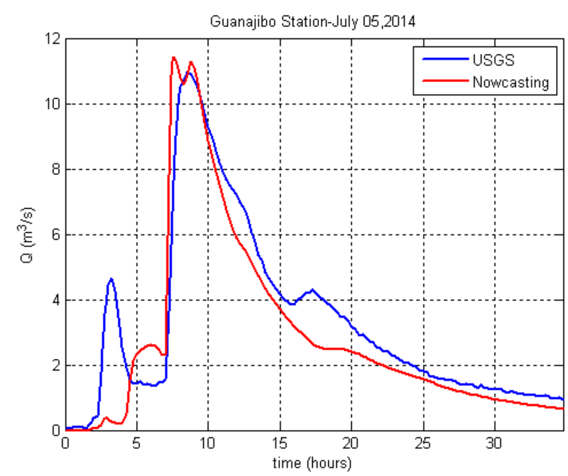

Figure 20. The runoff observed data (USGS) blue line and simulated data (Nowcasting) red line at Guanajibo station on July 05, 2014.

Figure 21 presents the comparison between data and observation on March 28, 2012, at Rosario station USGS.

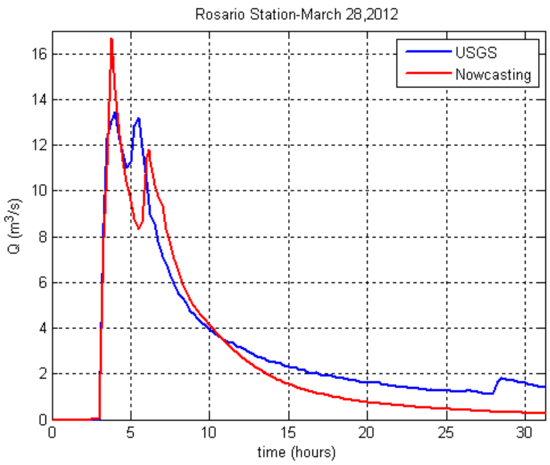

Figure 21. The runoff observed data (USGS) blue line and simulated data (Nowcasting) red line at Rosario station on March 28, 2012.

The probabilistic flood forecast developed in this research together with the inundation model are capable of providing a forecast of when and where river banks are likely to be overtopped. This could be more detailed with several cross sections into the river.

Decisions for evacuation can be categorized by determining the risk that overtopping represent to residents in areas adjacent to rivers or stream flows. The available knowledge when the evacuation decision can be made include probabilistic flood forecast published by each zone or location with large historical floods. Furthermore, it is then associated with the relevant topographical and demographical information for the basin and river, and the cost associated with the flooding and evacuation.

The approach of FAS (Flood Alert System) is to minimize loss of life and disruptions to communities through identification of the evacuation decision and strategy that has the maximum expected value under current conditions. The potential cost related with the decision model for evacuation can be categorized as losses resulting from preventable flood damage and losses from evacuation.

Inundation Analysis is a *Vflo* extension that provides images and animation showing the extent of forecast inundation, which can be used an indication of flood risk [*Vieux*, 2013].

To show the full potential of this tool in enhancing the visualization of the flood area, the program was run with a large storm data. Figure 22 presents a specific time for the basin area on March 28, 2012. The area north was the most affected by the rainfall on this event. Inundation Analysis presents an inundation sequence each hour. Other events were modeled using inundation animation.

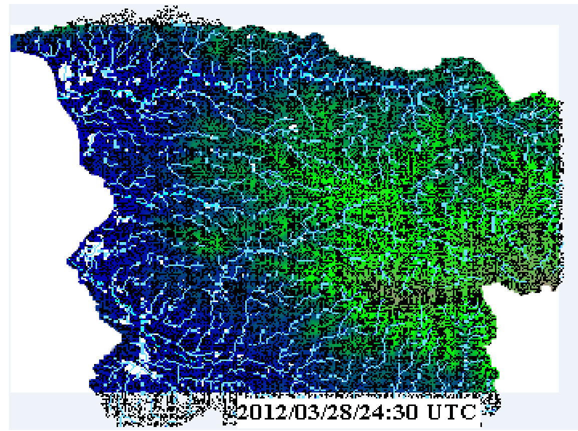

Figure 22. Inundation at specific time, on March 28, 2012.

9. Conclusion

This paper represents the first time that TropiNet radar technology has been used for hydrologic analyses and specifically for rainfall forecasting in Puerto Rico. Results from the nowcasting model at spatial and temporal scales demonstrated the capability of the model to reproduce observed rainfall, for each nowcasting lead-time with relatively good agreement.

The best statistical results were found in the rainfall nowcasting model with a lead-time of 10 min, as expected. It is well known that prediction of sudden storms using rainfall nowcasting models represent the category that are the most difficult to predict, and consequently, providing accurate flash flood warnings from these types of storms is a major challenge.

The nowcasting model has a limitation in the time shift because we are assuming that the cloud is a rigid object and that the cloud speed is constant, when in reality these parameters could vary. To find the actual weather conditions, more atmospheric parameters would need to be taken into account. In fact, cloud speed depends on its formation, and other physical parameters that are constantly changing [*Corfidi et al.*, 1996]. These factors should be taken into account in future works.

The major contribution of this research is the postulated model that represents the spatial and temporal variation of rainfall rates. Several parameter estimations were developed at each spatial and temporal domain, and the stochastic behavior of rainfall intensity was represented by an exponential time and spatial lag model, which is an approximation of a stochastic transfer function.

The algorithm searches for contiguous rain pixels and identifies rain cells in the last two radar images to estimate the cloud motion vector. This newly developed rainfall nowcasting algorithm was validated with ten (10) storms and results comparing the algorithm with observed data as well as the hydrological results showed that the nowcasting model is a suitable tool for predicting the most likely areas to become inundated.

Comparisons between rain gauges, TropiNet and NEXRAD demonstrated that the TropiNet radar system provides a higher degree of accuracy in rainfall estimation compared to NEXRAD.

This was the first attempt to evaluate a rainfall prediction in the western Puerto Rico area. The most hydrological sensitive parameter in the basin area is the initial saturation.

When the hydrologic model was evaluated within the Mayagüez bay drainage basin with three USGS reference stations, the San Sebastian station showed the highest flow. The events analyzed presented more rainfall in the north basin area.

The nowcasting model was evaluated with the available events from TropiNet radar, but it was develop to also work with events with high precipitation. Similarly, the hydrological model was evaluated in this study with relatively small flow (180 m^3/s), but could be evaluated with extraordinary events when they occur. Unfortunately, during the study period there were no high precipitation events.

ACKNOWLEDGEMENTS Financial support for this research was received from the NSF Collaborative Adaptive Sensing of the Atmosphere (CASA) Engineering Research Center (NSF Grant 0313747) and NOAA's Cooperative Remote Sensing Science and Technology Center (NOAA-CREST Grant 191 NA06OAR4810162).

10. REFERENCES

Corfidi, S. F., J. H. Merritt and J. M. Fritsch (1996). Predicting the movement of mesoscale convective complexes. *Wea. Forecasting*,11, 41-46.

Cruz-Pol, S., J. Colom, M. Córdoba, G. Pablos, J. Ortiz, W. Castellanos, M. Acosta, and J. Trabal (2011). Red de Radares Meteorológicos Desarrollados en el RUM. Revista. *Dimensión Ingeniería y Agrimensura CIAPR*., 25 (1), 13-17.

FEMA, (2012). Flood Insurance Study. *Commonwealth of Puerto Rico*, Volume 1 of 5, Preliminary: June. 22, 2012. Federal Emergency Management Agency.

French, M.N., W.F. Krajewski and R.R. Cuykendall (1992). Rainfall forecasting in space and time using a neural network. *J. Hydrol*., 137: 1-31.

Gourley, J.J., and B.E. Vieux (2005). A method for evaluating the accuracy of quantitative precipitation estimates from a hydrologic modeling perspective. *American Meteorological Society*. April, 115-133.

Marshall, J.S. and W. Palmer (1948). The distribution of raindrops with size. *J. Meteor.*, 5, 165-166.

Pielke, R.A., (1984): Mesoscale Meteorological Modeling. New York, N.Y.: *Academic Press*, 612 pp.

Ramírez-Beltran, N.D, Castro, J.M., Harmsen, and E. Vasquez, R. (2008). Stochastic transfer function models and neural networks to estimate soil moisture. *Journal of the American Water Resources Association*. Vol. 44, No. 4, pp 847-865.

Ramirez-Beltran, N.D., J. M. Castro, and J. Gonzalez (2014). An algorithm for predicting the spatial and temporal distribution of rainfall rate. *International Journal of Water*, in press.

Ramirez-Beltran, N.D., Torres-Molina, L., Castro, J.M., Cruz-Pol, S., Colom-Ustáriz, J.G. and Hosannah, N. (2015) 'A nonlinear regression model in the time and space domain for radar rainfall nowcasting', *Int. J. Hydrology Science and Technology*, Vol. 5, No. 3, pp.208–232.

Rojas, A.M., (2012). Flood Prediction Limitations in small watersheds with mountainous terrain and high rainfall variability. *Doctor of Philosophy in Civil Engineering*, University of Puerto Rico at Mayagüez , PR.

Trabal, J. M., G.A. Pablos-Vega, J.A. Ortiz, J.G. Colom-Ustáriz, S. Cruz-Pol, D.J. McLaughlin, M. Zink and V. Chandrasekhar (2011). Off-the-Grid Weather Radar Network for Precipitation Monitoring in Western Puerto Rico. *Proceedings of the International Symposium on Weather Radar and Hydrology*., Exeter, UK, April.

Toth, E., A. Brath, and A. Montanari (2000). Comparison of Short-term Rainfall Prediction Models for Real-Time Flood Forecasting, *Journal of Hydrology* 239, 132-147.

Torres-Molina, L.E., (2014). Flood Alert system Using Rainfall Data in The Mayagüez Bay Drainage

Basin, Western Puerto Rico. *Doctor of Philosophy in Civil Engineering*, University of Puerto Rico at Mayagüez , PR.

U.S. Census Bureau, (2010). Census 2010 Data for Puerto Rico. U.S. Census Bureau.

USDA, U.S. Department of Agriculture, Natural Resources Conservation Service, (2006a). *Soil Survey Geographic (SSURGO) database for Mayagüez area*. Puerto Rico Western Part, pr684, Fort Worth, Texas, Publication date: Dec. 26. URL:http://SoilDataMart.nrcs.usda.gov/

USDA, U.S. Department of Agriculture, Natural Resources Conservation Service, (2006b). *Soil Survey Geographic (SSURGO) database for Lajas Valley Area*. Puerto Rico, pr687 Fort Worth, Texas, Publication date: Dec. 26. URL:http://SoilDataMart.nrcs.usda.gov/

USDA, U.S. Department of Agriculture, Natural Resources Conservation Service, (2006c). *Soil Survey Geographic (SSURGO) database for Arecibo area*. Puerto Rico Western Part, pr682, Fort Worth, Texas, Publication date: Dec. 26. URL:http://SoilDataMart.nrcs.usda.gov/

USDA, U.S. Department of Agriculture, Natural Resources Conservation Service, (2006d). *Soil Survey Geographic (SSURGO) database for Ponce area*. Puerto Rico Western Part, pr688, Fort Worth, Texas, Publication date: Dec. 26. URL:http://SoilDataMart.nrcs.usda.gov/

U.S Geological Survey -Current Water Data for Puerto Rico (2014) http://waterdata.usgs.gov/pr/nwis/rt

Vieux, B.E. and J.E. Vieux (2002). *Vflo* ™: A real-time distributed hydrologic model. *Proceedings of the Second Federal Interagency Hydrologic Modeling Conference,* July 28-August 1, Las Vegas, NV 2002. Abstract and paper in CD-ROM.

Vieux, B.E. and F.G. Moreda (2003). Ordered physics-based parameter adjustment of a distributed model In: Duan, Q., Sorooshian, S., Grupta, H.V., Rousseau, A.N., Turcotte, R. (Eds.), *Water Science and Application Series*, vol. 6. American Geophysical Union, pp. 267-281, ISBN 0-87590-355-X (Chapter 20).

Vieux, B.E., 2013, Vieux, INC. GIS, Hydrology and Radar rainfall, viewed 12 January 2013, <http://www.vieuxinc.com>.

Westrick, K. J., C. F. Mass, and B. A. Colle (1999). The limitations of the WSR-88D radar network for quan-titative precipitation measurement over the costal western United States. *Bull. Amer. Meteor. Soc*.